High Order Discontinuous Galerkin Method for Elastohydrodynamic Lubrication Line Contact Problems

H. Lu, M. Berzins, C. E. Goodyer and P. K. Jimack*

School of Computing, University of Leeds, LS2 9JT, U.K.

SUMMARY

In this paper a high order Discontinuous Galerkin method is used to solve steady-state isothermal line contact elastohydrodynamic lubrication problems. This method is found to be stable across a wide range of loads and is shown to permit accurate solutions using just a small number of degrees of freedom provided suitable grids are used. A comparison is made between results obtained using this proposed method and those from a very large finite difference calculation in order to demonstrate excellent accuracy for a typical highly loaded test problem. Copyright © 2000 John Wiley & Sons, Ltd.

KEY WORDS: elastohydrodynamic lubrication; discontinuous Galerkin; finite element method

1. INTRODUCTION

In most complex mechanical systems lubricants are used to reduce friction and protect moving parts against wear. In many cases, the geometry of the contacting elements determines the shape of the lubricant film. However, in the cases of concentrated contacts such as journal bearings and gears, the contacting elements deform elastically defining the film thickness: this is known as elastohydrodynamic lubrication (EHL). Numerical solutions of EHL are very important for industry in the design and evaluation of both lubricants and components. These cases require the simultaneous solution of both pressure and film thickness, along with the behaviour of the lubricant under these extreme conditions.

The key features of an EHL solution are the low pressure inlet region; a rapid rise in pressure through the centre of the contact, typically reaching the giga-Pascal range; a cavitation boundary in the outflow; and, a sharp pressure spike passed the centre of the contact, towards the outflow. It has been shown that if this spike is not resolved sufficiently well then the calculated friction can be inaccurate [1].

The finite difference (FD) method is perhaps the most widely used numerical solution method. Stability through wide ranges of operating conditions has been attained through use of the different FD techniques in the low and high pressure regions, as shown by Venner [2]

---

*Correspondence to: pkj@comp.leeds.ac.uk

and Nurgat *et al.* [3]. In order to accelerate convergence the multigrid method was first employed by Lubrecht in 1986 [4]. For the fast calculation of the elastic deformation Brandt and Lubrecht [5] developed a multilevel multi-integration algorithm which significantly reduces the computational complexity in approximating deformations at each point in the contact. Based on the above achievements, FD combined with multigrid [2, 6, 7] has become the most popular method for EHL problems since it is both efficient and stable.

Other techniques for EHL are also used. The inverse method of [8], which is mainly suitable for highly loaded cases, updates the pressure profile from film thickness rather than the other way around. The coupled method of [9, 10] calculates the pressure and film thickness simultaneously instead of iterating between them and can be applied with either FD or FE (finite element) discretizations. The FE method has also been successfully used to solve incompressible EHL contact problems by a number of authors, e.g. [11, 12, 13]. For compressible EHL contact problems, upwinding is necessary in order to ensure stability. For example, in [9], oscillations are observed in the central region in highly loaded cases when using a traditional quadratic finite element method to discretize the problem

In recent years the Discontinuous Galerkin (DG) method has become a popular choice for solving convection-dominated partial differential equations [14, 15, 16]. Since discontinuity is allowed over element interfaces, we get the opportunity to stablize the high-order method by defining an appropriate numerical flux. DG can easily handle irregular meshes and the degree of the approximating polynomial can be easily changed from one element to another. In this paper, high-order DG is used to solve smooth EHL line contact problems. Our numerical experiments show that this approach can give very accurate solutions with only a small number of unknowns: for example results obtained using less than 200 unknowns are shown to be comparable to FD results obtained using over half a million equally spaced points.

2. GOVERNING EQUATIONS

The mathematical model of line contact EHL problems typically consists of three equations, shown here using the usual non-dimensionalization, described fully in [6]. The Reynolds equation reads

$$\frac{\mathrm{d}}{\mathrm{d}X}\left(\epsilon\frac{\mathrm{d}P}{\mathrm{d}X}\right) - \frac{\mathrm{d}(\rho H)}{\mathrm{d}X} = 0, \tag{1}$$

where $\epsilon = \frac{\rho H^3}{\eta\lambda}$, P and H are the unknown pressure and film thickness, ρ and η are the density and viscosity, and λ is a dimensionless speed parameter. (The lubricant rheology is highly non-linear in pressure: in this work we have used the viscosity-pressure relationship of Roelands [17] and density model of Dowson and Higgison [18].) The elasticity is included through the film thickness equation which defines the contact geometry for a given pressure solution:

$$H(X) = H_{00} + \frac{X^2}{2} - \frac{1}{\pi}\int_{-\infty}^{\infty}\ln|X - X'|P(X')\,\mathrm{d}X'. \tag{2}$$

The force balance equation is a conservation law for the applied load, given by:

$$\int_{-\infty}^{\infty}P(X)\,\mathrm{d}X - \frac{\pi}{2} = 0. \tag{3}$$

For physical reasons, all pressures should be larger than or equal to the vapour pressure of the lubricant (zero). This is not accounted for in the Reynolds equation, hence, in the outlet region, the calculated solution may have negative pressures. Consequently the Reynolds equation is only valid in the pressurized region and, the cavitation position, X_{cav}, is therefore treated as a free boundary. The boundary conditions are:

$$P(X_{in}) = 0, \quad P(X_{cav}) = 0 \quad \text{and} \quad \frac{\mathrm{d}P}{\mathrm{d}X}(X_{cav}) = 0, \tag{4}$$

where X_{in} denotes the inlet boundary position, located far enough from the contact region to approximate an infinite boundary.

3. DISCONTINUOUS GALERKIN DISCRETIZATION

This section demonstrates the application of the DG method for the discretization of the above equations.

3.1. The Reynolds Equation

The Reynolds equation can be written in the following general form in both the 1D (considered here) and 2D cases:

$$-\nabla \cdot (\epsilon \nabla P) + \nabla \cdot (\beta \rho H) = 0, \tag{5}$$

where $\beta = 1$ in 1D and $\beta = (1,0)$ in 2D. Let $\mathcal{P}_h$ be a partition of the domain Ω into N elements Ω_e. On each internal interface $\Gamma_{int} = \partial \Omega_e \cap \partial \Omega_f$ with $e > f$ we have the normal n_e pointing from Ω_e to Ω_f. Let Γ_D be the Dirichlet boundary where $P = g$ and Γ_- be the inflow part of the boundary. Here g is the solution on the Dirichlet boundary and for EHL line contact problems $g = 0$. We define the jump of a function v on the element interface Γ_{ef}

$$[v]_{ef}(x) = v|_{\partial \Omega_e \cap \Gamma_{ef}} - v|_{\partial \Omega_f \cap \Gamma_{ef}}, \ e > f, \tag{6}$$

and the average

$$\langle v(x) \rangle_{ef} = \frac{1}{2}(v|_{\partial \Omega_e \cap \Gamma_{ef}} + v|_{\partial \Omega_f \cap \Gamma_{ef}}). \tag{7}$$

Following the approach of [14] and [15], a discrete form of the Reynolds equation becomes:

$$a(P, v) = l(P, v), \tag{8}$$

where

$$a(P, v) = \sum_{\Omega_e \in \mathcal{P}_h} \left(\int_{\Omega_e} \nabla v \cdot \epsilon \nabla P \, \mathrm{d}x \right) + \int_{\Gamma_{int}} ([P]\langle (\epsilon \nabla v) \cdot n \rangle - [v]\langle (\epsilon \nabla P) \cdot n \rangle) \, \mathrm{d}s$$

$$+ \int_{\Gamma_D} (P(\epsilon \nabla v) \cdot n - v(\epsilon \nabla P) \cdot n) \, \mathrm{d}s, \tag{9}$$

and

$$l(P, v) = \sum_{\Omega_e \in \mathcal{P}_h} \left(\int_{\Omega_e} (\nabla v \cdot \beta) \rho H \, \mathrm{d}x \right) - \int_{\partial \Omega_e \setminus \Gamma_-} v(\rho(P^-)H)(\beta \cdot n_e) \, \mathrm{d}s$$

$$- \int_{\Gamma_-} v\rho(g)H(\beta \cdot n) \, \mathrm{d}s + \int_{\Gamma_D} (\epsilon \nabla v) \cdot ng \, \mathrm{d}s. \tag{10}$$

In the above equations,

$$P^- = \lim_{\delta \to 0} P(x - \delta\beta), \text{ for } x \in \Gamma_{int} \tag{11}$$

and n is the outer unit normal and $n = n_e$ on Γ_{int}.

In each element, P is expressed in the following form:

$$P^e = \sum_{i=1}^{p^e+1} u_i^e N_i^e, \tag{12}$$

where p^e is the order of the approximating polynomial, u_i^e are the unknown coefficients and N_i^e are the local basis functions. The discontinuous basis functions used here are described in [19]. Note that in (10) upwinding is easily implemented by picking the left value $\rho(P^-)$ when calculating the numerical flux (see the third term in (10)).

3.2. The Film Thickness Equation

For a given pressure distribution the film thickness may be calculated as follows:

$$
\begin{aligned}
H(X) &= H_{00} + \frac{X^2}{2} - \frac{1}{\pi} \int_{X_{in}}^{X_{cav}} \ln|X - X'| P(X') \, dX' & \text{(13a)} \\
&= H_{00} + \frac{X^2}{2} - \frac{1}{\pi} \sum_{e=1}^{N} \int_{\Omega_e} \ln|X - X'| P(X') \, dX' & \text{(13b)} \\
&= H_{00} + \frac{X^2}{2} - \frac{1}{\pi} \sum_{e=1}^{N} \int_{\Omega_e} \ln|X - X'| \sum_{i=1}^{p^e+1} u_i^e N_i^e(X') \, dX' & \text{(13c)} \\
&= H_{00} + \frac{X^2}{2} - \frac{1}{\pi} \sum_{e=1}^{N} \sum_{i=1}^{p^e+1} \int_{\Omega_e} \ln|X - X'| N_i^e(X') \, dX' \, u_i^e & \text{(13d)} \\
&= H_{00} + \frac{X^2}{2} - \frac{1}{\pi} \sum_{e=1}^{N} \sum_{i=1}^{p^e+1} K_i^e(X) u_i^e, & \text{(13e)}
\end{aligned}
$$

where the $K_i^e(X)$ are defined by:

$$K_i^e(X) = \int_{\Omega_e} \ln|X - X'| N_i^e(X') \, dX'. \tag{14}$$

Here $K_i^e(X)$ is calculated using numerical integration: for $X \in e$ singular quadrature is employed since $\ln|X - X'|$ has a weak singularity at $X' = X$; elsewhere Gaussian quadrature is satisfactory.

3.3. The Force Balance Equation

The force balance equation is discretized according to:

$$\sum_{e=1}^{N} \int_{\Omega_e} \sum_{i=1}^{p^e+1} u_i^e N_i^e(X) \, dX - \frac{\pi}{2} = 0. \tag{15}$$

4. SOLUTION PROCEDURE

This section describes a simple solution procedure that may be used on a given mesh and with a given choice of the polynomial degree on each element.

The underlying relaxation scheme assumes that if X_{cav} is given then the discrete form of (8), along with the first two conditions in (4), may be written in the general form:

$$L(U) = A(U)U - b(U) = 0, \tag{16}$$

where $U = (u_1^1, \ldots, u_{p^1+1}^1; \ldots; u_1^N, \ldots, u_{p^N+1}^N)$ are the unknown pressure coefficients. Note that both $A(U)$ and $b(U)$ depend on U. The pressure is relaxed according to:

$$U \leftarrow U + \left(\frac{\partial L}{\partial U}\right)^{-1} R, \tag{17}$$

where R is the residual of the discrete Reynolds equation and $\frac{\partial L}{\partial U}$ is approximated by:

$$\frac{\partial L}{\partial U} \approx A(U) - \frac{\partial b(U)}{\partial U} \tag{18}$$

which is a full matrix since $H(X)$ has a global pressure integral.

The cavitation position, X_{cav}, must be chosen so as to impose the third condition in (4). This is achieved by moving the entire grid according to the current value of $\frac{\mathrm{d}P}{\mathrm{d}X}(X_{cav})$: if $\frac{\mathrm{d}P}{\mathrm{d}X} > 0$ the grid is moved left and if $\frac{\mathrm{d}P}{\mathrm{d}X} < 0$ the grid is moved right. The displacement, dx, is defined by:

$$dx = -\delta \frac{\mathrm{d}P}{\mathrm{d}X}(X_{cav}), \tag{19}$$

where δ is a small positive constant.

The above ingredients are used within the following overall solution procedure.

(i) Start with an initial choice of X_{cav} and an initial pressure distribution.
(ii) Relax H_{00} using the error in equation (15), as explained in [6] for example.
(iii) Compute the thickness profile $H(X)$ from (13e).
(iv) Update the pressure distribution by repeating (18) until convergence.
(v) Update the cavitation position according to the value of $\frac{\mathrm{d}P}{\mathrm{d}X}(X_{cav})$.
(vi) Return to step (ii) until the converged solution with $\frac{\mathrm{d}P}{\mathrm{d}X}(X_{cav}) = 0$ is obtained.

5. NUMERICAL RESULTS

In this section we demonstrate the potential of the DG method by comparing solutions for a high load test problem against those obtained using a standard multi-level, multi-integration FD algorithm. It is shown in [1] that in order to fully resolve the pressure spike up to half a million FD grid-points may be required. Here we compare our DG results against increasing resolutions of FD grids. For the DG solution 16 elements are used (not of equal size) and the polynomial degree is either 10 (in the pressure spike region) or 8 (elsewhere).

Figure 1 shows the pressure profile computed for a typical highly loaded case. The entire contact is shown in the left graph whilst a detailed view of the position of the pressure spike
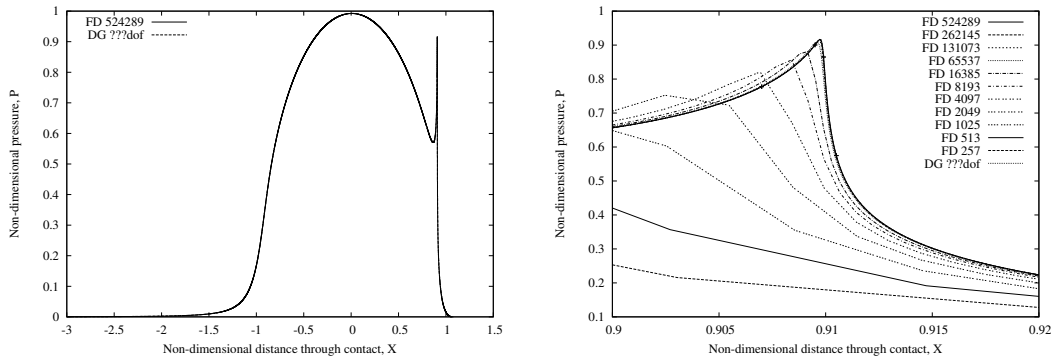
Figure 1. Pressure distributions obtained using DG and FD methods across the entire contact, left, and around the pressure spike, right

Method	Unknowns	Peak Pressure	Peak Position	Free Boundary Position
FD	4097	0.8212	0.9069	1.0693
FD	8193	0.8566	0.9084	1.0701
FD	16385	0.8810	0.9092	1.0704
FD	65537	0.9095	0.9066	1.0705
FD	131073	0.9138	0.9097	1.0707
FD	262145	0.9158	0.9097	1.0706
FD	524289	0.9164	0.9097	1.0706
DG FE	168	0.9169	0.9097	1.0707

Table I. Comparsion of Pressure Peak Position and Free Boundary Values

is shown on the right. The key features of interest are the peak value of pressure, its position and the point at which the free boundary occurs. These values are shown in Table 1. It is clear from these results that the DG solution is closest to the half million point FD results.

Note that solution efficiency is not considered in this communication. The FD calculations would obviously benefit from the use of locally refined meshes, such as used in [1, 20], whilst the DG method could certainly be implemented with a more efficient solution algorithm (based upon p-multigrid, [21] for example). What has been demonstrated however is that the DG approach can deliver very high accuracy using only a small number of degrees of freedom.

6. DISCUSSION

In this paper a high order DG algorithm is used to solve the EHL line contact problem for the first time and, unlike for traditional (continuous) FE methods, stability is easily obtained through the use of a simple upwinding step. Our numerical results show that, when suitable grids are used, highly accurate solutions may be obtained with very few degrees of freedom, thus illustrating the exciting potential of this approach for the solution of EHL problems. Other results of similar quality have been obtained under different loading conditions and using different solution algorithms (e.g. the penalty method described in [22]).

Copyright © 2000 John Wiley & Sons, Ltd.
Prepared using cnmauth.cls

Commun. Numer. Meth. Engng 2000; 00:1–6

For the results obtained in this paper a very crude adaptive strategy was used to select the mesh and the local polynomial degree. Currently we are investigating more sophisticated h-p-refinement strategies for this method. We are also in the process of developing a multigrid version of the solution algorithm based upon the p-multigrid method, described in [21] for example, and will also consider 2-d point contact cases.

REFERENCES

1. Goodyer CE, Fairlie R, Hart DE, Berzins M, and Scales LE. Calculation of Friction in Steady-State and Transient EHL Simulations In A. Lubrecht *et al.*, editor, *Transient Processes in Tribology: Proceedings of the 30th Leeds-Lyon Symposium on Tribology.* Elsevier, 2004.
2. Venner CH. *Multilevel Solution of the EHL Line and Point Contact Problems.* PhD thesis, University of Twente, Netherland, 1991.
3. Nurgat E, Berzins M and Scales LE Solving EHL problems using iterative, multigrid and homotopy methods. *J. Tribol-T ASME*, **121**: 28–34, 1999.
4. Lubrecht AA, Ten Napel WE, Bosma R. Multigrid, an alternative method for calculating film thickness and pressure profile in elastohydrodynamically lubricated line contacts. *J. Tribol-T ASME*, **108**: 28–34, 1986
5. Brandt A, Lubrecht AA. Multilevel matrix multiplication and fast solution of integral equations. *J. Comput. Phys.*, **90**: 348–370, 1990
6. Venner CH, Lubrecht AA. *Multilevel Methods in Lubrication.* Elsevier, 2000.
7. Jing Wang, Shiyue Qu, Peiran Yang. Simplified multigrid technique for the numerical solution to the steady-state and transient EHL line contacts and the arbitrary entrainment EHL point contacts. *Tribology International*, **34**: 191–202, 2001.
8. Kweh CC, Evans HP, Snidle RW. Elastohydrodynamc lubrication of heavily loaded circular contacts. *P. I. Mech. Eng. C-J MEC*, **203**: 133–148, 1989.
9. Hughes TG, Elcoate CD, Evans HP. A novel method for integrating first- and second-order differential equations in elastohydrodynamic lubrication for the solution of smooth isothermal, line contact problems. *Int. J. Numer. Meth. Eng.*, **44**: 1099–1113, 1999.
10. Elcoate CD, Evans HP, Hughes TG. On the coupling of the elastohydrodynamic problem. *P. I. Mech. Eng. C-J MEC*, **212**: 307–318, 1998.
11. Taylor C, O'Callaghan J F. A numerical solution of the elastohydrodynamic lubrication problem using finite elements. *J. Mech. Eng. Science.* **14**: 229–237, 1972.
12. Rohde S M, Oh K P. A unified treatment of thick and thin file elastohydrodynamic problems by using higher order element methods. *Proc. R. Soc. Lond. A.* **343**: 315–331, 1975.
13. Wu S R, Oden J T. A note on application of adaptive finite elements to elastohydrodynamic lubrication problems. *Commun. Apllied Numer. Meth.* **3**: 485–494, 1987.
14. Oden JT, Babuska I and Baumann CE. A discontinuous hp finite element method for diffusion problems. *J. Comput. Phys.* **146**: 491–519, 1998.
15. Baumann CE, Oden JT. A discontinuous hp finite element method for diffusion problems. *Comput. Methods. Appl. Mech. Engrg.* **175**: 311–341, 1998.
16. Cockburn B, Karniadakis GE, Shu CW. *Discontinuous Galerkin Methods: Theory, Computation and Applications.* Springer, 1999.
17. Roelands CJA, Vlugter JC, Watermann HI. The viscosity temperature pressure relationship of lubricating oils and its correlation with chemical constitution. *ASME J. Basic Engng.* **85**: 601, 1963.
18. Dowson D, Higginson GR. *Elasto-hydrodynamic Lubrication, The Fundamentals of Roller and Gear Lubrication.* Permagon Press, Oxford, Great Britain, 1966.
19. Szabo B, Babuska I. *Introduction to Finite Element Analysis.* John Wiley and Sons, Inc, 1989.
20. Goodyer CE, Fairlie R, Berzins M, and Scales LE. Adaptive mesh methods for elastohydrodynamic lubrication. In *ECCOMAS CFD 2001 : Computational Fluid Dynamics Conference Proceedings.* Institute of Mathematics and its Applications. ISBN 0-905091-12-4, 2001.
21. Fidkowski KJ, Darmofal DL. Development of a higher-order solver for aerodynamic applications. *42nd AIAA Aerospace Sciences Meeting and Exhibit, AIAA Paper 2004-0436*, 2004.
22. Wu SR. A penalty formulation and numerical approximation of the Reynolds-Hertz problem of elastohydrodynamic lubrication. *Int. J. Engng. Science.* **24**: 1001–1013, 1986.